PERGAMON

International Journal of Solids and Structures 40 (2003) 3463–3476

INTERNATIONAL JOURNAL OF SOLIDS and STRUCTURES

www.elsevier.com/locate/ijsolstr

Damage model with delay effect Analytical and numerical studies of the evolution of the characteristic damage length

Arnaud Suffis [a,c], Ton A.A. Lubrecht [b], Alain Combescure [a,*]

[a] *Laboratoire de Mécanique des Solides, INSA de Lyon, Bat. 304, 20 avenue Albert Einstein, Villeurbanne Cedex 69621, France*
[b] *Laboratoire de Mécanique des Contacts, UMR 5514, INSA de Lyon, Bat. J. d'Alembert, 20 avenue Albert Einstein, 69621 Villeurbanne Cedex, France*
[c] *Laboratoire d'Etude de Dynamique, Commisariat à l'Energie Atomique—Saclay, 91191 Gif-Sur-Yvette Cedex, France*

Received 8 July 2002; received in revised form 14 February 2003

Abstract

This paper studies the delayed damage model in a one-dimensional transient analysis. It is well-known that kind of model prevents the mesh dependency when it is used in a finite element code. The model problem concerns a clamped uniaxial damage elastic bar submitted to a step load at its extremity. In order to guarantee the correct behaviour of the model and to be able to choose the appropriate mesh size before performing a finite element calculation, an analytical evaluation of the size of the damaged zone called characteristic length is given and compared to the converged numerical results. Finally, a two-dimensional example is treated with a damage with or without the delay effect.

Keywords: Damage model; Characteristic length; Finite element; Transient analysis; Delay effect

1. Introduction

Classical damage models used in numerical analysis suffer from mesh dependence and usually lead to localization of the deformation into a single element. The mesh dependency is a well-known problem that is encountered for example with strain-softening materials and several models exist that avoid the dependency on the mesh. One could quote in particular the non-local model, the rate-dependent model or the gradient-dependent plasticity model (Bazant and Pijaudier-Cabot, 1998; de Borst et al., 1990; Needleman, 1988).

This paper focuses on a model developed at the ''Laboratoire de Mécanique et de Technologie de Cachan'' amongst others by Allix and Deü (1997), Allix et al. (1999), Deü (1997) and Ladevèze (1991) named delayed damage model where a delay effect is introduced. Considering that the classical damage models allow the damage rate to increase indefinitely, the original idea was to introduce a limitation of the

* Corresponding author. Tel.: +33-4-72-43-6426; fax: +33-4-72-43-85-78.
E-mail address: alain.combescure@insa-lyon.fr (A. Combescure).

0020-7683/03/$ - see front matter
doi:10.1016/S0020-7683(03)00153-7

damage rate in the damage evolution law. Until now, the previous authors have always limited the use of this model to composite laminates, although the damage rate limitation can also solve the localization phenomenon for simpler materials as elastic material with damage or any other material with damage (Suffis and Combescure, 2002).

The aim of this study is to allow the choice of an appropriate mesh size for numerical analysis of this type of model. The present paper focuses on the one-dimensional problem and to some extent on the two-dimensional problem. It is organised as follows. The first part of this paper analyses the delayed damage model in order to underline its main properties and, in particular, its ability to solve the localization problem. Whereas Deü has studied the fracture duration in detail, this analysis addresses the fracture size in order to choose the appropriate mesh size for the calculation. This process requires an approximation of the fracture size to be known a priori, otherwise several calculations will be necessary to chose the right mesh. An analytical pre-determination of the fracture size close enough of the exact solution allows one to choose immediately the appropriate refinement. For a one-dimensional example, an analytical characteristic length has been calculated with a simplified delayed damage model and the results have been compared to the numerical solutions; this development is presented in a second part. The next part validates the one-dimensional method by comparing the analytical curves with the numerical results. Moreover, a numerical analysis of the order of accuracy of the delayed damage model was carried out to validate the numerical results. Finally, two-dimensional examples treated with or without the delayed damage model are presented.

2. Delayed damage model

This section presents the delayed damage model and the analysis is limited to the case of an elastic damage material (even if it can be applied to several types of materials (Suffis and Combescure, 2002)). As stated in Section 1, classical damage models are mesh dependent. So, firstly, the main equations and properties of the damage model without delay effect are described (Allix et al., 1999; Chaboche and Lemaitre, 1996). Then, a one-dimensional example is treated in order to show the localization phenomenon. Next, a characteristic time which is the foundation of the delayed damage model will be introduced (Allix and Deü, 1997; Allix et al., 1999; Ladevèze et al., 2000); model equations are then presented and results of numerical simulations are given.

The central difference algorithm is used to integrate explicitly the equation of motion (Hugues, 1987). Without the non-linearities introduced by the delayed damage model, it guarantees a second-order accuracy with respect to the time. Simulations are performed with an element of constant size Δx. The central difference method is conditionally stable; thus, there exists a critical time step Δt_{crit} beyond which the calculation diverges. For a one-dimensional problem, Δt_{crit} corresponds to the time for an elastic wave to pass through an element. Hereafter, the time step is taken equal to the critical one (it is generally chosen equal to the critical one multiplied by a safety factor). We will see in Section 4.2, how the convergence order is conserved even if the delayed damage model is used when the mesh and hence the time step are both reduced.

For the examples treated in this part and all those which will follows (except when specified otherwise), the material parameters are taken equal to $E = 57$ GPa, $\rho = 2280$ kg/m^3 (so that the wave velocity inside the material is equal to $c = 5000$ m/s), $Y_0 = 0$ MPa, $Y_c = 0.23$ MPa.

2.1. Classical damage model

2.1.1. Classical damage evolution law

The study is limited to a one-dimensional example of a bar subjected to tension. This model was first proposed by Bazant and Pijaudier-Cabot (1998) for analysing the mesh dependency phenomenon on strain-

softening materials. The material is elastic; the Young's modulus is noted E and the density ρ. There is only one variable representing the damage, it varies from 0, for an undamaged material, to 1, for a fully damaged one, and is noted D. The damage evolution is driven by the damage energy release rate Y (which is deduced from the strain energy density E_D) and the damage is taken linear from a threshold value Y_0 to a critical one Y_c. We could note that, in our case, the damage energy release rate is proportional to stress and also to strain. Moreover, damage can only increase and this increase is possible only under tensile stress conditions which open cracks, enabling their growth. This distinction between tension and compression leads one to consider only the positive part of the stress (denoted by $\langle\cdot\rangle$) when defining Y. The complete equations are given in Eq. (1). Two types of stress appear in these equations; the classical stress σ which corresponds to the macroscopically measured quantity and the effective stress σ_{eff} which correspond to a microscopic quantity (Lemaitre, 1996). This last stress is linear as a function of the strain.

It is important here to point out that the stress versus strain curve obtained for a zero-dimensional example (single element clamped on one side and with an imposed displacement on the other) is independent of the strain rate, so that the same curve is obtained whatever the imposed velocity.

$$\begin{cases} \sigma_{\text{eff}} = E\varepsilon \\ \sigma = (1-D)\langle\sigma_{\text{eff}}\rangle - \langle-\sigma_{\text{eff}}\rangle = E(1-D)\langle\varepsilon\rangle - E\langle-\varepsilon\rangle \\ E_D = \dfrac{1}{2}\left[\dfrac{\langle\sigma\rangle^2}{E(1-D)} + \dfrac{\langle-\sigma\rangle^2}{E}\right] \\ Y = \left.\dfrac{\partial E_D}{\partial D}\right|_{\sigma=\text{Cst}} = \dfrac{\langle\sigma\rangle^2}{2E(1-D)^2} = \dfrac{E\langle\varepsilon\rangle^2}{2} \\ f(Y) = \dfrac{\sqrt{Y}-\sqrt{Y_0}}{\sqrt{Y_c}-\sqrt{Y_0}} \\ \begin{cases} D = \langle \sup_{\tau\leqslant t}(f(Y_\tau))\rangle & \text{if } d<1 \\ D = 1 & \text{otherwise} \end{cases} \end{cases} \tag{1}$$

2.1.2. Dynamic analysis for a bar

We consider here the classical problem of a bar of 0.1 m in length under tension clamped at one extremity and subjected to an imposed displacement or load on the other (Bazant and Pijaudier-Cabot, 1998), Fig. 1 gives its description. A similar configuration is obtained with a strip submitted to simple shearing (Needleman, 1988). It is convenient to avoid wave reflection. Therefore, loadings are chosen so that rupture appears on the free extremity of the bar. We observe that rupture happens as soon as the limit of stability (i.e. $D = 0.5$) is reached in a single element and then, rupture (i.e. $D = 1$) occurs in this element whatever the size of the mesh (see Fig. 2). This phenomenon reflects a mesh dependence. Indeed the size of the localized zone is always reduced to one element. Mathematical considerations of this problem are not treated in this

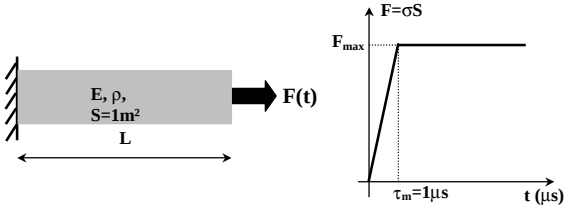

Fig. 1. One-dimensional bar in tension, imposed load on the right side (one could as well impose the displacement).

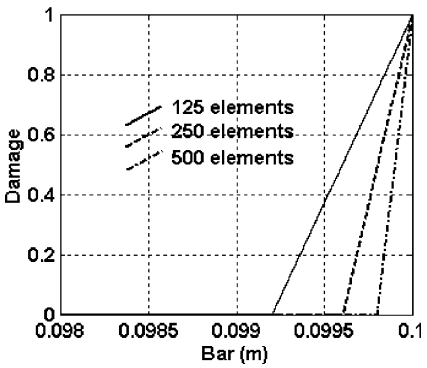

Fig. 2. Damage profile along the bar. Results for different meshes (zoom on the right extremity) without delay effect. Damage is confined into a single element.

paper, but some authors like De Borst have studied this aspect (de Borst et al., 1990). Besides, the damage reaches 1 in only one element once the limit of stability is exceeded. It means in particular that rupture occurs immediately after this event (in one time step) whatever the loading velocity and the size of the mesh. So, the smaller the time step, the higher the damage rate. This observation led Deü (1997) to introduce a delay effect in the damage.

2.2. The delay effect

2.2.1. Fundamental equation

As stated before, the damage rate is not limited when the mesh is refined. It tends towards infinity. Physically, this characteristic seems to make little sense. Indeed, there must be a characteristic damage evolution which defines a limitation of the damage rate. This idea was the basis of the delayed damage model first proposed by a team of the "Laboratoire de Mécanique et de Technologie de Cachan" within the framework of the studies on the rupture of composite laminates (Allix and Deü, 1997; Allix et al., 1999; Deü, 1997). In the model developed, two parameters are introduced. One is the characteristic time τ_c representing the inverse of the maximum damage rate. The equation of the damage rate evolution reads:

$$\begin{cases} \dot{D} = \frac{1}{\tau_c}[1 - \exp(-a\langle f(Y) - D\rangle)] & \text{if } D < 1 \\ D = 1 & \text{otherwise} \end{cases} \tag{2}$$

where a is the second parameter of the model. One observes the classical definition of damage without delay $f(Y)$. The damage rate is calculated from the difference between this classical damage without delay and the damage D with delay effect. In this way, a fast variation of the damage energy release rate will not lead to an immediate evolution of the damage. The damage will evolve with a certain delay fixed by the characteristic time independent of the mesh.

The immediate consequence is that, for the stress versus strain curve of a zero-dimensional example, the higher the strain rate, the higher the maximum stress (Allix et al., 1999; Deü, 1997). Indeed, the limitation of the damage rate allows the stress to increase more than in a classical model, so that the nearest element will damage when several elements are used.

2.2.2. Dynamic analysis for a bar

The example presented in Fig. 1 is studied again, but now with an imposed displacement. Fig. 3a shows the final damage along the bar with a length of 0.1 m meshed with n elements and a strain rate at the

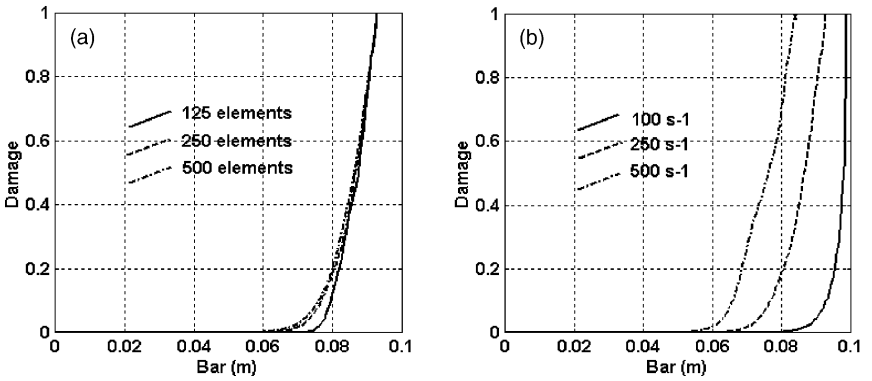

Fig. 3. Damage profile along the bar. (a) The results for different meshes (the fully damaged zone is approximately 9 mm) with delay effect. (b) The evolution of the length of the fully damaged zone with strain rate with delay effect.

extremity of 250 s^{-1}. The damage parameters used for this simulation are $\tau_c = 2$ μs and $a = 10$ and Y_0 is here chosen equal to 0.05 MPa. Several simulations have been realised, modifying only the mesh size and hence the step time. The following conclusions can be drawn:

- the damaged zone is not confined to a single element (characteristic of the mesh dependency phenomenon),
- the size of the damage zone is independent of the mesh,
- the profile of the damage along the bar is independent of the mesh,
- the energy dissipated in the bar is constant whatever the mesh.

All these conclusions show that the delayed damage model guarantees a solution independent of the mesh .

Additional simulations have been performed with several velocities (Fig. 3b); the same conclusions are obtained. However, the size of the fully damage zone (i.e. the zone where the damage is equal to 1) evolves with the velocity. The higher the strain rate imposed at the extremity of the bar, the larger the size of the fully damage zone. This conclusion is coherent with the results obtained for a single element (Allix et al., 1999; Deü, 1997). Indeed, when the strain rate increases, the stress increases more than with a classical model and more elements are damaged. That means in particular that if one is able to determine approximately the fracture length a priori, one would be able to chose the appropriate mesh. The next part deals with the analytical determination of the fracture length for a one-dimensional problem.

2.2.3. Choice of parameters

In this paper, it is supposed that the parameters τ_c and a are known. Different sets of parameters have been chosen for each example in order to show that the model works for a large range of parameters.

The identification of the two parameters can be performed using specific tests. For example, Sen Gupta investigated a 3D Carbon/Carbon laminate (Allix and Sen Gupta, 2001; Sen Gupta, 2001) from an experimental stress versus pulse width curve obtained with plate impact experiments (Goeke and McClintock, 1975).

3. Analytical determination of the characteristic length

The exact analytical solution of the full problem has not been found, although all the constitutive equations are known. It is necessary to simplify the damage evolution law to determine a coherent

characteristic fracture length. The study will be confined to the front of the stress wave. This section details the simplification made in the damage evolution law, then an analytical length is calculated as a function of a critical stress which will be defined in a later paragraph.

3.1. Simplification of the damage evolution law

The classical damage evolution law with delay effect introduced by Deü (1997) reads for an elastic damage material:

$$\dot{D} = \frac{1}{\tau_c}(1 - \exp(-a\langle f(Y) - D\rangle)) \quad \text{if } D < 1,\ D = 1 \text{ otherwise} \tag{3}$$

with

$$f(Y) = \frac{\sqrt{Y} - \sqrt{Y_0}}{\sqrt{Y_c} - \sqrt{Y_0}} \quad \text{and} \quad Y = \frac{\sigma^2}{2E} \tag{4}$$

The study is limited to what happens just after the front of the stress wave passed. Thus, damage is initiating at that point and hence $D \approx 0$. The function h of x expressing the damage rate in front of the stress wave can be written as follows:

$$h(x) = \frac{1}{\tau_c}(1 - \exp(-a\langle x\rangle)) \tag{5}$$

We approximate this function by a Heaviside function with values 0 and $1/\tau_c$. A critical stress (hence a critical damage energy release rate) fixes the boundaries of each domain. This critical value has to be chosen with care (see Section 3.3). Eq. (6) summarises this simplification.

$$\dot{D} = \frac{1}{\tau_c} \quad \text{if } \sigma \geqslant \sigma_{\text{crit}},\ \dot{D} = 0 \text{ otherwise} \tag{6}$$

3.2. Analytical characteristic length

The example presented in Fig. 1 is studied once more. The load applied to the bar is a step (the rise time τ_m is zero), the stress step is denoted by $\Delta\sigma$.

The equations which govern the behaviour of the bar read:

$$\begin{cases} \sigma_{\text{eff}}(x,t) = E\varepsilon(x,t) \\ \varepsilon(x,t) = \dfrac{\partial u(x,t)}{\partial x} \\ \sigma(x,t) = (1 - D(x,t))\sigma_{\text{eff}}(x,t) \\ \dfrac{\partial \sigma(x,t)}{\partial x} = \rho \dfrac{\partial^2 u(x,t)}{\partial t^2} \end{cases} \tag{7}$$

where x and t denote respectively the space variable and time and where the damage D follows the simplified evolution law described by Eq. (6). One can combine these equations and deduce a second-order differential equation that is only a function of the effective stress and the damage (see Eq. (8)).

$$\frac{\partial^2(\sigma_{\text{eff}}(x,t)(1 - D(x,t)))}{\partial x^2} = \frac{\rho}{E}\frac{\partial^2 \sigma_{\text{eff}}(x,t)}{\partial t^2} = \frac{1}{c^2}\frac{\partial^2 \sigma_{\text{eff}}(x,t)}{\partial t^2} \tag{8}$$

Eq. (8) can be rewritten as follows:

$$\lim_{\mathrm{d}x\to 0}\left[\frac{1}{\mathrm{d}x^2}(\sigma_{\mathrm{eff}}(x+\mathrm{d}x,t)(1-D(x+\mathrm{d}x,t))-2\sigma_{\mathrm{eff}}(x+\mathrm{d}x,t)(1-D(x+\mathrm{d}x,t))\right.$$
$$\left.+\sigma_{\mathrm{eff}}(x+\mathrm{d}x,t)(1-D(x+\mathrm{d}x,t)))\right]=\frac{1}{c^2}\lim_{\mathrm{d}t\to 0}\left[\frac{1}{\mathrm{d}t^2}(\sigma_{\mathrm{eff}}(x,t+\mathrm{d}t)-2\sigma_{\mathrm{eff}}(x,t)+\sigma_{\mathrm{eff}}(x,t-\mathrm{d}t))\right] \quad (9)$$

As interest is limited to the solution on the wave front, the following relations between space and time are considered:

$$\begin{cases} x=ct \\ \mathrm{d}x=c\,\mathrm{d}t \end{cases} \quad (10)$$

where c is the wave velocity in the non-damaged material. One can first remark that stress and damage are zero before the wave front passes at point $x=ct$; this leads to:

$$\begin{cases} \sigma_{\mathrm{eff}}(x+c\,\mathrm{d}t,t)=0 \\ \sigma_{\mathrm{eff}}(x,t-\mathrm{d}t)=0 \\ D(x+c\,\mathrm{d}t,t)=0 \end{cases} \quad (11)$$

Introducing now the simplified damage model (see Eq. (6)), one can deduce:

$$\begin{cases} D(x,t)=0 \\ D(x-c\,\mathrm{d}t,t)=\dfrac{\mathrm{d}t}{\tau_{\mathrm{c}}} \end{cases} \quad (12)$$

Inserting Eqs. (11) and (12) in Eq. (9), the differential equation becomes:

$$\begin{cases} \dfrac{\mathrm{d}\sigma_{\mathrm{eff}}(t)}{\mathrm{d}t}+\dfrac{1}{\tau_{\mathrm{c}}}\sigma_{\mathrm{eff}}(t)=0 \\ \sigma_{\mathrm{eff}}(0)=\Delta\sigma \quad \text{(initial condition)} \end{cases} \quad (13)$$

where $\sigma_{\mathrm{eff}}(t)$ represents the effective stress just behind the front of the stress wave. The solution of the differential equation (13) reads:

$$\sigma_{\mathrm{eff}}(t)=\Delta\sigma\exp\left(-\frac{t}{\tau_{\mathrm{c}}}\right) \quad (14)$$

This solution remains true until $\sigma_{\mathrm{eff}}\geqslant\sigma_{\mathrm{crit}}$ (condition expressed in Eq. (6)). Hence, we can derive a limit time:

$$t_{\mathrm{lim}}=\tau_{\mathrm{c}}\ln\left(\frac{\Delta\sigma}{\sigma_{\mathrm{crit}}}\right) \quad (15)$$

Multiplying the two sides of Eq. (15) by the wave velocity in the non-damaged material, we deduce a characteristic length:

$$L_{\mathrm{c}}=c\tau_{\mathrm{c}}\ln\left(\frac{\Delta\sigma}{\sigma_{\mathrm{crit}}}\right) \quad (16)$$

In Eq. (15), a critical stress σ_{crit} appears. It is not defined yet, but one can already see its importance. A study of a discrete model with the same simplification has been performed (Suffis and Combescure, 2002). Initially, a small dependency on the mesh was obtained, but the length rapidly converges towards the analytical result when the mesh is refined.

3.3. Critical stress

Using the result of Eq. (16), two analytical values of the critical stress can be obtained from the numerical results. A minimum critical stress will correspond to a maximum characteristic length and a maximum critical stress will correspond to a minimum characteristic length.

The minimum critical stress must be equal to the stress leading to a damage initiation in the full delayed damage law (see Eq. (17)).

$$\sigma_{\text{crit}}^{\min} = \sqrt{2EY_0} = \sigma_0 \tag{17}$$

The maximum critical stress is given by Eq. (18):

$$\sigma_{\text{crit}}^{\max} = \sqrt{2EY_0} + 3\frac{\sqrt{2EY_c} - \sqrt{2EY_0}}{a} = \sigma_0 + 3\frac{\sigma_c - \sigma_0}{a} \tag{18}$$

It corresponds to the stress leading approximately to a damage rate equal to 95% of the maximum damage rate $1/\tau_c$ in an initially non-damaged material.

4. Numerical analysis for a one-dimensional example

Up to now, only the consequences on the time until fracture have been explored (Deü, 1997). This part focuses on the comparison of the numerical fracture length and the analytical one. Then, the similarities of numerical and experimental results are pointed out. In the mean time, the influence of the parameters on the characteristic length can be studied. Finally, the convergence of the model is analysed, and some results are given for the one-dimensional bar.

4.1. Numerical characteristic length

4.1.1. Comparison between analytical and numerical results

First, the measurement of the characteristic length using the numerical results must be clarified; it corresponds to the length for which damage is exactly equal to 1 at the end of the calculation. The calculations were stopped when the damage did no longer evolve. As the wave reflection must be avoided to identify the characteristic length without ambiguity, the length of the bar was chosen such that this last condition was satisfied. For the example treated in Section 2.2.2, the characteristic length is around 9 mm (see Fig. 3a).

The evolution of the characteristic length versus the stress step is plotted in Fig. 4. The delayed damage parameters a and τ_c are respectively equal to 10 and 5 μs. The results are independent of the mesh re-

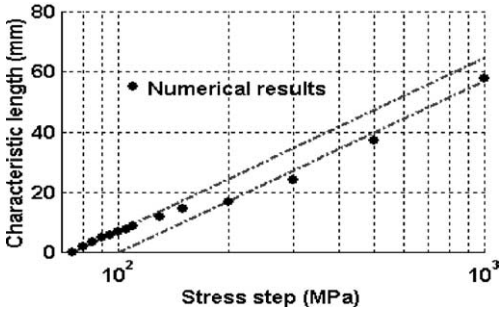

Fig. 4. Characteristic length versus stress step (logarithm), numerical results and analytical boundaries.

finement under the condition that elements are small enough to capture the fracture. The minimum stress required for fracture is linked to the value of the damage release rate threshold Y_0; in this case, σ_0 is equal to 75.5 MPa. One can observe a very good correlation between analytical and numerical characteristic length. Fig. 4 shows in particular that the numerical results follow the upper boundary $L_c^{0\%}$ for loadings near the threshold stress σ_0. For more severe loadings, the evolution of the characteristic length remains linear with the same slope, but is closer to the lower boundary. Again one can find the same behaviour for each numerical analysis whatever the delayed damage parameters and the material parameters (Suffis and Combescure, 2002).

In conclusion, this analysis allows one to observe that the analytical model fits the numerical results. It permits an excellent prediction of the fracture length in the case of a one-dimensional bar.

4.1.2. Influence of damage model parameters

The influence of the damage model parameters clearly appears in Eqs. (16)–(18). A variation of the characteristic time τ_c involves a similar variation of the slope of the characteristic length versus the stress step curves $L_c^{0\%}$ and $L_c^{95\%}$ (with a logarithmic scale for stress). A variation of the parameter a influences only the maximum stress (see Eq. (18)); it does not affect $L_c^{0\%}$ and induces a variation of the distance between $L_c^{0\%}$ and $L_c^{95\%}$. Deü, who studied this influence in terms of fracture duration has already given an interpretation of the parameter a which is larger for 'brittle' materials than for 'ductile' ones (Allix et al., 1999). As stated before, the numerical results are in good agreement with the analytical one whatever the delayed damage parameters. Thus, one can conclude that the parameters have the same influence in the numerical model as in the analytical model. The detailed result are presented in Suffis and Combescure (2002).

4.2. Convergence analysis

This part studies the influence of the mesh refinement on the accuracy. As the time step follows the Courant condition (i.e. the time step corresponds to the time required for the wave passing through the smallest element of the structure multiplied by a safety factor), refining the mesh generates a decrease of the time step by the same amount. So, the convergence with respect to time and space is analysed simultaneously. If the algorithm is first-order accurate with respect to 'time and space', dividing the mesh (and thus the time step) by two generates a division of the error by a factor of two; if it is second-order, the error is divided by four and so on and so forth... Thus the accuracy order can be determined with the help of numerical simulations on the one-dimensional bar as follows:

$$\frac{X^1 - X}{X^2 - X} = \frac{\mathrm{O}((\Delta x)^k)}{\mathrm{O}((\Delta x/2)^k)} = \frac{\mathrm{O}((\Delta t)^k)}{\mathrm{O}((\Delta t/2)^k)} = 2^k \tag{19}$$

where X^1 refers to a quantity calculated with a coarse mesh, X^2 with a mesh twice finer, X is the exact solution and k is the order of accuracy which can be thus deduced. As the exact solution X is a priori unknown, it is impossible to determine the error this way. Nevertheless, the difference between two successive levels of refinement (the mesh of reference represents level 1, level $i+1$ corresponds to a mesh refined 2^i times) will give the same result. The two first simulations give the first difference ΔX_i between level i and level $i+1$, then ΔX_{i+1} between level $i+1$ and level $i+2$ is calculated. The ratio $R = \Delta X_i/\Delta X_{i+1}$ is equal to 2^k.

$$\left.\begin{aligned} &\frac{X^i - X^{i+1}}{X^{i+1} - X^{i+2}} = \frac{(X^i - X) + (X - X^{i+1})}{(X^{i+1} - X) + (X - X^{i+2})} = \Delta R \\ &X^i - X = \mathrm{O}((\Delta x/2^{i-1})^k) = \mathrm{O}((\Delta t/2^{i-1})^k) \end{aligned}\right\} \Rightarrow \Delta R = 2^k \tag{20}$$

As this study focuses on damage, the error in terms of damage and in terms of displacement are estimated. The example of the one-dimensional bar of Fig. 1 is used again. The load applied at the extremity of the bar is such that damage occurs but no rupture. The first numerical experiment was made with a bar meshed with 32 elements corresponding to level 6. The material parameters are the same as those used in Section 2.2.2 except for the delayed damage model parameters (i.e. $E = 57$ GPa, $\rho = 2280$ kg/m^3, $a = 5$, $\tau_c = 5$ μs, $Y_0 = 0.05$ MPa and $Y_c = 0.23$ MPa). The bar is 0.05 m in length and the calculation is done for 10 μs with a time step equal to half the critical time step. During the first half of the calculation, the load applied grows linearly until it reaches 50 MN and it then remains constant until the end of the calculation (i.e. $F_{max} = 50$ MN and $\tau_m = 30$ μs in Fig. 1).

Fig. 5a and b shows respectively the difference between successive levels for damage and displacement at the end of the calculation. The displacements are compared at the common nodes between the two successive levels. Moreover, each element of level i is divided in two elements to generate level $i+1$. The damage difference is calculated between each element of level i and the average of the two corresponding elements of level $i+1$. One can remark the noise which disturbs the results and the amplitude of the oscillations which decreases when the level increases. That is why the convergence is sometimes quite difficult to observe graphically. Thus, the integral of the difference between the two levels along the bar is given in Table 1. Similar results can be obtained by integrating the difference with respect to time; indeed, these results are available for each time t and then for the integral with respect to time.

The conclusion one can draw from this analysis is that the order of accuracy is equal to 2. This result can also be found by refining mesh and time step in two separate steps. The first and the second step show without ambiguity the second-order accuracy with respect to time and with respect to space respectively

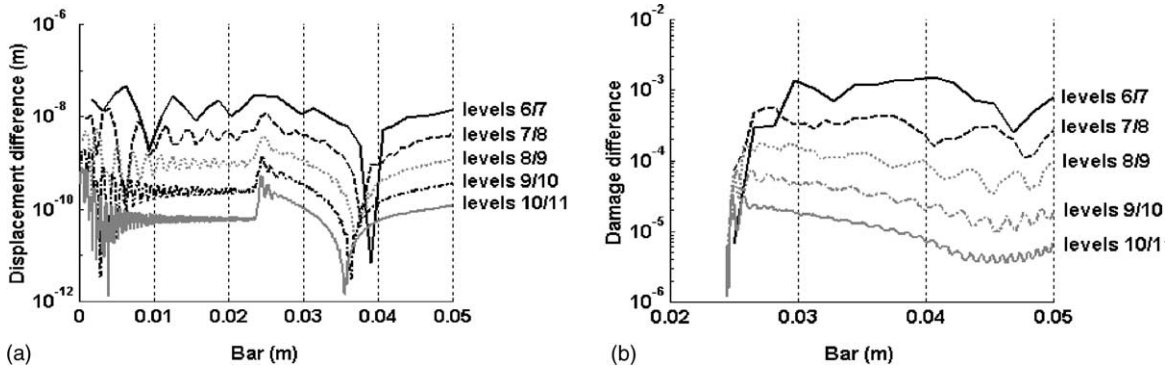

Fig. 5. Difference in the solution (logarithmic scale) between two levels along the bar. (a) The difference between the successive levels in terms of displacement. (b) The difference between successive levels in terms of damage.

Table 1
Integral of the difference along the bar between the successive levels in terms of displacement and damage and corresponding ratio

Level i	Displacement		Damage	
	$\Delta U_i = U^i - U^{i+1}$	$\Delta U_i/\Delta U_{i+1}$	$\Delta D_i = D^i - D^{i+1}$	$\Delta D_i/\Delta D_{i+1}$
6	3.73e−10	3.73	1.14e−5	2.92
7	1.00e−10	3.65	3.91e−6	3.16
8	2.74e−11	3.52	1.24e−6	3.04
9	7.78e−12	3.35	4.07e−7	2.76
10	2.32e−12	–	1.47e−7	–
11	–	–	–	–

Table 2
Integral of the difference in term of displacement along the bar

Level i $\Delta t = 2.44$ ns	Displacement		Time step $N = 32$	Displacement	
	$\Delta U_i = U^i - U^{i+1}$	$\Delta U_i/\Delta U_{i+1}$		$\Delta U_i = U^i - U^{i+1}$	$\Delta U_i/\Delta U_{i+1}$
Panel a			*Panel b*		
6	3.64e−10	3.59	$\Delta t_{crit}/2$	2.01e−10	3.85
7	1.01e−10	3.59	$\Delta t_{crit}/4$	5.22e−11	3.97
8	2.82e−11	3.50	$\Delta t_{crit}/8$	1.31e−11	4.17
9	8.07e−12	3.27	$\Delta t_{crit}/16$	3.15e−12	4.01
10	2.46e−12	–	$\Delta t_{crit}/32$	7.87e−13	–
11	–	–	$\Delta t_{crit}/64$	–	–

Panel a compares the successive levels with a constant step time. Panel b compares the successive time steps with a constant mesh.

(Table 2 (Panels a and b) show the difference between two successive levels in the two cases for the displacement only). Whatever the convergence condition, this analysis shows that the results of the calculation converge towards a stable solution with the mesh refinement and this convergence is second-order accurate.

4.3. Conclusions

With the two last paragraphs, one can henceforth conclude that the characteristic length for a one-dimensional problem is well known. The analytical model developed in Section 3 predicts a characteristic length that is close to the one observed numerically. Furthermore, the numerical solution is second-order accurate.

5. Rupture computations

In this section, two-dimensional examples are treated. The classical example is the case described in Fig. 6 of a horizontal beam blocked at the left extremity and subjected to a vertical step load on the right extremity. The load is equally distributed over the nodes of the right side. The computation was performed with different meshes detailed later. A first set of simulations allows one to compare the behaviour of the classical damage model and the delayed damage model for a two-dimensional problem.

An explicit finite-element code was specifically developed for the calculation performed hereafter; the post-processing is realised with the help of Gmsh (Geuzaine and Remacle, 2002). The beam is meshed with quadrangular elements with four points of integration (Hugues, 1987; MacNeal, 1994). The material studied in this section is elastic ($E = 57$ GPa, $\nu = 0.3$, $\rho = 2280$ kg/m^3) with damage. The classical damage (without addition of the delay effect) is isotropic and follows a linear law with respect to the sum of the squares of the positive part of main deformations between a threshold value ε_0 equal to 0.0011 and a critical value ε_c equal to 0.0034. The delay parameters are $\tau_c = 10$ μs and $a = 1$. The hypothesis of plane strain is made.

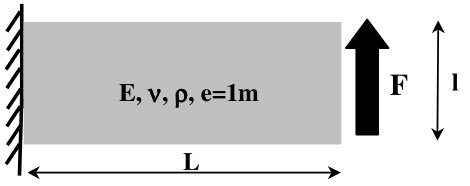

Fig. 6. Two-dimensional bending beam, imposed load on the right.

The calculation was performed with a beam of 0.1 by 0.04 m with unit thickness, for a load of 0.8 MN and a total time of 0.25 ms. Once again, the solution on several levels is compared. It is important to note that the increase of one level results in a division of a quadrangular element in four small quadrangular elements; indeed, each side of the initial element Δx and Δy is divided by two. The damage profiles at the end of the calculation are depicted in Fig. 7a–c for a material without delay effect and in Fig. 8a–c for a material with delay effect. The lower level correspond to a beam meshed with 20 by 10 elements and the following levels correspond respectively to a beam meshed with 40 by 20 elements and 80 by 40 elements.

The classical damage model gives results which are clearly dependent on the mesh size. For all three meshes, the damage initiates at the bottom of the beam where the stress due to the bending exceeds the threshold stress corresponding to ε_0. Then the damage evolves quickly until complete rupture. The 'crack' propagates vertically from this point until it 'bifurcates' in several 'cracks' which seem to evolve arbitrarily

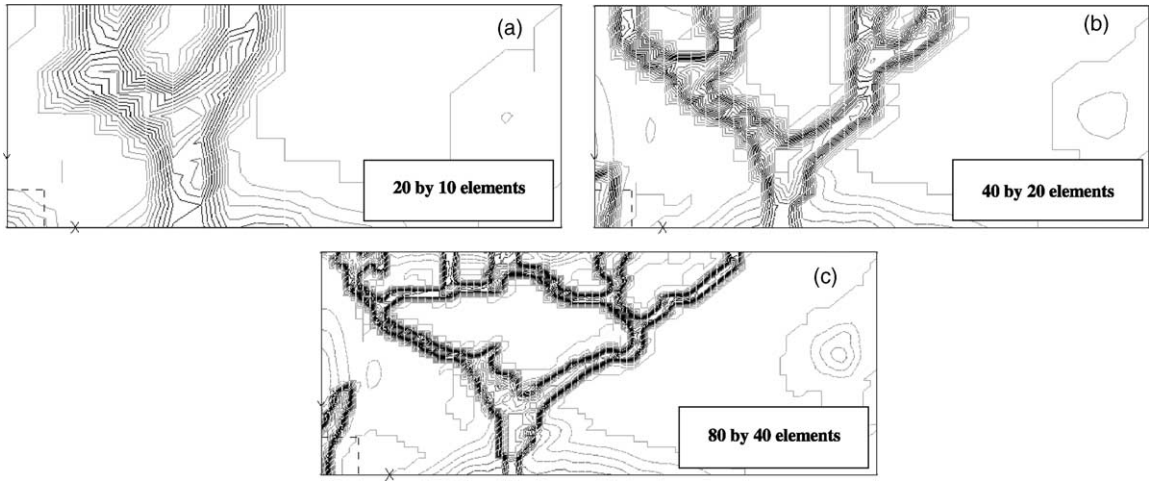

Fig. 7. Damage profiles in a beam without delay effect.

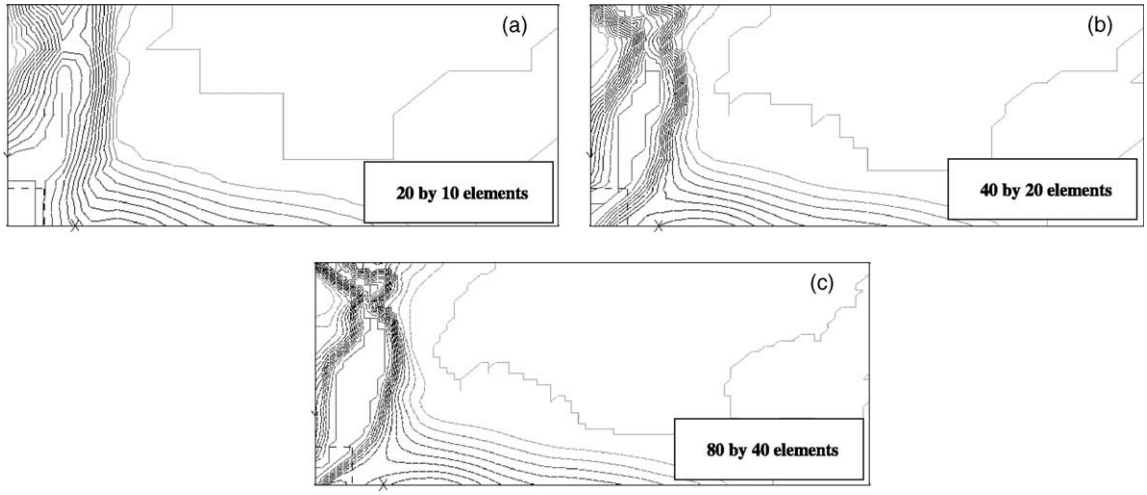

Fig. 8. Damage profiles in a beam with delay effect.

depending on the mesh used. One can note that what we call 'crack' corresponds in fact of a continuum line of fully damaged elements. The thickness of this line is always one element independent of the mesh. This mesh dependency represented by this unitary thickness and this arbitrarily evolution is highlighting the mesh dependency phenomenon. Concerning the results obtained with the delayed damage model, one can notice that the profiles of damage are similar for each level. Like the simulations without delay effect, the damage initiates at the bottom of the middle of the beam, but it does not lead to rupture. As the damage evolution is slowed down by the delay, the rupture only occurs when the wave reflects on the extremity. A fully damage zone, the profile of which remains constant independent of the mesh, appears at the bottom of the beam and propagates vertically until complete rupture.

6. Conclusions

The first sections of this paper illustrated the essential properties of the delayed damage model. An original approach was then presented, the aim of which is to analyse the delayed damage model in terms of a characteristic length. The first step made above is contained in the analytical one-dimensional model which allows one to evaluate beforehand the fully damaged zone and thus to choose the appropriate mesh refinement. The validation of the analytical model was performed by comparing its predictions with the numerical results. Furthermore, the second-order accuracy was demonstrated and hence one can affirm that the analytical results are in total agreement with the numerical ones.

As an introduction to the studies to come, two-dimensional examples are presented. Once again, the delayed damage model gives satisfactory results as it avoids the mesh dependency phenomenon.

Another possible extension is the generalisation of the model to any material with damage. Several classes of materials have already been treated (Suffis and Combescure, 2002) and the model seems to be adaptable to all damage materials as it only requires a small extension to the existing models. However, before the delayed damage model can be applied to a new 'material', one has to measure the parameters a and τ_c experimentally.

References

Allix, O., Deü, J.F., 1997. Delay-damage modelling for fracture prediction of laminated composites under dynamic loading. Eng. Trans. 45, 29–46.

Allix, O., Deü, J.F., Ladevèze, P., 1999. A delay damage meso-model for prediction of localisation and fracture of laminates subjected to high rates loading. ECCM 99.

Allix, O., Sen Gupta, J., 2001. Composite damage mesomodel for impact problems: application to 3D C/C material. ECCM 2001.

Bazant, Z.P., Pijaudier-Cabot, G., 1998. Local and non-local models for strain-softening, and their comparison based on dynamics analysis. In: Cracking and Damage. Elsevier Applied Science, Cachan, France, pp. 379–390.

Chaboche, J.L., Lemaitre, J., 1996. Mécanique des matériaux solides. Dunod, Paris.

de Borst, R., Mülhaus, H.-B., Pamin, J., Sluys, L.J., 1990. Computational modelling of localisation of deformation. In: Luxmoore, A.R., et Owen, D.R.J. (Eds.), Proc. Third Int. Conf. Computational Plasticity. University of Swansea, UK, pp. 483–508.

Deü, J.F., 1997. Rupture des composites stratifiés sous chargement dynamique: apports des méso-modèles avec endommagement retardé. Thèse de doctorat, Ecole Normale Supérieure de Cachan, Laboratoire de Mécanique et de Technologie de Cachan.

Geuzaine, C., Remacle, J.F., 2002. Gmsh: a three dimensional finite element mesh generator with built-in pre- and post-processing facilities, available from internet: <URL:http://www.geuz.org/gmsh>.

Goeke, E.C., McClintock, F.A., 1975. Fracture of graphite composite under shock loading. J. Appl. Phys. 46 (11), 4671–4673.

Hugues, T.R.J., 1987. The Finite Element Method: Linear Static and Dynamic Finite Element Analysis. Prentice Hall.

Ladevèze, P., 1991. About a damage mechanics approach. In: Batiste, D. (Ed.), Mechanics and Mechanisms of Damage in Composites and Multi-materials. London, pp. 119–141.

Ladevèze, P., Allix, O., Deü, J.F., Léveque, D., 2000. A mesomodel for localisation and damage computation in laminates. Comp. Meth. Appl. Mech. Eng. 183, 105–122.

Lemaitre, J., 1996. A Course on Damage Mechanics. Springer, Paris.
MacNeal, R.H., 1994. Finite Element: Their Design and Performance. Marcel Dekker Inc., New York.
Needleman, A., 1988. Material dependance and mesh sensitivity in localization problems. Comp. Meth. Appl. Mech. Eng. 67, 69–86.
Sen Gupta, J., 2001. Analyse du comportement sous choc d'un composite 3D Carbon/Carbone. Mémoire de DEA, Laboratoire de Mécanique et de Tehnologie de Cachan, Ecole Normale Supérieure de Cachan.
Suffis, A., Combescure, A., 2002. Modèle d'endommagement à effet retard: étude numérique et analytique de l'évolution de la longueur caractéristique. REEF 02, 11, 593–619.